Engineering and Technology Journal
Journal homepage: https://etj.uotechnology.edu.iq

Theory and Modeling of Slab Waveguide Based Surface Plasmon Resonance

Amnh S. Hasan, Razi J. Al-Azawi, Ali A. Alwahib*

Laser and Optoelectronics Engineering Dept., University of Technology-Iraq, Alsina'a Street, 10066 Baghdad, Iraq.
*Corresponding author Email: ali.a.alwahib@uotechnology.edu.iq

HIGHLIGHTS

- Adding the graphene layer at different thicknesses increases the electric field in the refractive index range.
- Increasing Graphene thickness directly affected the increasing loss.
- Sensitivity for sensor-based Graphene is always crucial for any applications which increase with increasing graphene thickness.

ARTICLE INFO

Handling editor: Evan T. Salim

Keywords:

Surface plasmon resonance, waveguide, Graphene, silver.

ABSTRACT

The current study proposes a developing surface plasmon resonance (SPR) sensor that has been widely employed to detect viruses, such as environmental analytes, biological and chemical analytes, and monitoring and medical diagnostics. Optical waveguides have much potential for developing new chemical and biological sensors. Graphene is the world's most vital substance and can be used to enhance other materials. A composite silver film-based SPR sensor with the waveguide. To enhance the silver film's stability, detect the best thickness with the best resonance using different types of analyte: air than 1.1, 1.2, 1.3, and water. The resonance wavelength numerically calculated, loss, sensitivity, Figure of merit FOM, and Refractive index using Lumerical FDE. The numerical data showed the differences in the electric field of SPR in the number of refractive indexes after applying the silver coating layer, and the performance parameters improved. Moreover, Graphene has much promise, yet almost most of it is still unexplored. The fundamentals of graphene-based waveguides and devices were investigated using two layers with FDE. The primary purpose of this study is to show the effective thickness of the Graphene and the analyte's refractive index to get high absorption.

1. Introduction

The development of advanced instruments in sensor application has become a critical problem in meeting demands and requirements of time control, short response time, miniature components, and real-time analysis [1]. Because of the substantial influencing factors and the difficulties of measuring their influence experimentally, SPR modeling and computer simulation are essential in optimizing and identifying optimal sensor conditions.

One of the many extant detecting devices, commonly known as "sensors," is based on a physical phenomenon known as surface plasmon resonance (SPR). This sort of sensor is popular nowadays because of its ability to respond quickly in real-time and without the need for labeling [2,3].

Since the initial surface plasmon resonance sensor in 1982, SPR sensing technology has advanced significantly. As a result, the SPR has been widely employed for detecting viruses, environmental analytes, biological and chemical analytes, and monitoring and medical diagnostics [4,5].

Surface plasmons (SPs) are a coherent oscillation of free electrons at the metal/solution interface. Surface plasmon has two categories: propagating surface plasmons (PSPs) and localized surface plasmons (LSPs) [6].

PSPs can be excited on metallic films using a variety of methods, including the Kretschman [7]and Otto [8] prism couplers, optical waveguides couplers [9], diffraction gratings [10], and optical fiber couplers [11]. In contrast, LSPs can be excited on metallic nano-particles, and both can substantially enhance electromagnetic fields in the near-field region (resonance amplification), leading to modern SPR [12].

Chemical sensor and biosensor technologies with high throughput are required in various fields, including life sciences, drug research, medical diagnostics, and food safety and security [13]. Surface Plasmon Resonance (SPR) biosensors are optical

http://doi.org/10.30684/etj.2022.132295.1100
Received 23 November 2021; Accepted 1 March 2022; Available online 10 July 2022
2412-0758/University of Technology-Iraq, Baghdad, Iraq

sensors the resonant coupling of electromagnetic waves to the charge density oscillations at the interface of dielectrics and metals [14]. In addition, optical waveguides can develop new chemical and biological sensors [15].

Waveguides are essential for communication and computer applications since they are resistant to electromagnetic interference, generated crosstalk, and diffraction[16]. Using the waveguides in sensors has several advantages, including compact size, durability, the ability to realize several optical functions on a single chip (integration with other optical components), and multichannel sensing [17]. Due to their flexibility and excellent noise immunity, optical sensor systems based on waveguides are greatly interested [18]. The strip-loaded waveguide is formed by loading a planar waveguide with a dielectric strip of index n2 < n1 or a metal strip to facilitate optical confinement in the y-direction. The film plane's planar waveguides with additional lateral waveguides are called strip waveguides [19]. There are two types of channel waveguides based on the shape, and the size of the film deposited onto the substrate, such as Graphene to work as a sensor. The detection limit of this type of sensor is directly connected to the value of the refractive index of waveguides, which is one of the most significant characteristics of waveguide sensors [20].

Graphene is the world's most vital substance, and it can be used to enhance other materials' characteristics. Graphene is a flat monolayer of carbon atoms tightly packed into a two-dimensional (2D) honeycomb lattice with sp2-hybridized carbon. It has gotten much press because of its potential uses in optoelectronics and containing carbon in a densely packed hexagonal structure, thermal conductivity, mechanical properties, and low band conductance [21]. Furthermore, the additional graphene layer on the silver metal protects the silver film and dielectric layer [22].

In 2006, Ong *et al*. suggested a waveguide surface plasmon resonance (SPR) optical sensor based on wavelength modulation MicroChem's SU-8 photoresist via UV lithography was used to fabricate Strip waveguides for exciting surface plasmon resonance. A bimetallic silver-gold film is deposited on the waveguides. They noticed overlying gold ensures that the stability of the metallic film is not compromised. In addition, they found the double-layer configuration possesses better sensitivity than the single gold film SPR configuration proposed configuration, as weighed against a single silver film, makes it a much better option for biosensing applications [23].

In 2009, Akowuah *et al*. proposed a novel planar waveguide SPR sensor based on the Otto configuration. Using an eigenmode solver, they have shown the sensor sensitivity of 4300 nm/RIU by selecting appropriate structural parameters [24]. The proposed waveguide SPR sensor has the analyte between the core and gold layers.

In 2016, MICLOŞ1 *et al.* studied Surface plasmon propagation in a multilayer planar waveguide structure. They proposed an algorithm for solving the characteristic equation to determine the complex effective refractive index n_{eff}. This study changed their approach to modeling plasmon propagation in planar waveguides, finding an absolute minimum by mesh refining. The algorithm proposed to simulate the surface plasmon propagation proved effective and accurate; they found that it provides a practical, accurate, and effective tool for designing waveguides for surface plasmons [25].

In 2020, JI *et al*. suggested designing a waveguide coupled surface plasmon sensor to detect liquid with a high refractive index (RI) based on polymer materials using the finite difference method. First, they studied the effects of variation in the thickness of the Au film, polymethyl methacrylate (PMMA) buffer, and waveguide layer on the waveguide's sensing performance. Then, they found that a thinner gold film gives rise to a more sensitive structure. At the same time, the variation in the thickness of the PMMA buffer and waveguide layer has a negligible effect on the sensitivity. However, the FOM of the sensor can be tuned effectively by the thicknesses of the PMMA buffer and waveguide layer. When the RI of liquid increases from 1.45 to 1.52, the sensitivity reaches 4518.14 nm/RIU [26].

In 2020, Kong *et al.* proposed a novel SPR sensor consisting of Graphene and subwavelength silver gratings using COMSOL Multiphysics commercial software based on the finite element method (FEM). The performance of the proposed SPR sensor was investigated, the researcher showed. The proposed sensor had excellent linearity between the resonance angle and refractive index in the range between 1.333 and 1.360, and the narrow FWHM (about 3.5 deg) the results showed could be obtained by optimizing the geometrical parameters. Also, they study the influence of the number of graphene layers on sensitivity. As a result, the designed sensor's maximum sensitivity reached 192 deg/refractive index unit (RIU) [27].

This study proposes a robust coupling method between a surface plasmon waveguide and Graphene. A graphene sheet was coated on the silver surface in the conventional SPR biosensor air and an aqueous environment.

2. Theory Equations

In the situation of an incident wave, consider the polarization considerations of the TE (s) or TM (p) light, in addition to taking into account the relations of the incident light Figure on an interface separating two dielectrics. Continuity in z = 0 interfaces). The electromagnetic fields define four reflection and transmission coefficients rs and rp, ts, and tp [28].

$$r_j = \frac{E^r_{c_j}}{E^i_{c_j}} \tag{1}$$

$$t_j = \frac{E^T c_j}{E^i c_j} \tag{2}$$

For the polarization TE (s):

$$r_s = \frac{n_c \cos\theta_0 - n_m \cos\theta_m}{n_c \cos\theta_{0+n_m} \cos\theta_m} \tag{3}$$

$$t_s = \frac{2n_c \cos\theta_0}{n_c \cos\theta_{0+n_c \cos\theta_m}} \quad (4)$$

For the polarization TM (p):

$$r_s = \frac{n_c \cos\theta_{m-}n_m \cos\theta_c}{n_c \cos\theta_m + n_m \cos\theta_c} \quad (5)$$

$$t_s = \frac{2n_c \cos\theta_0}{n_c \cos\theta_m + n_m \cos\theta_0} \quad (6)$$

3. Methodology

The Theoretical Modeling of the proposed sensor principle was designed from a composite silver film-based SPR sensor with a strip waveguide. The configuration was done on the FDE code for the dimensions [29] is used to excite SPR mode, as shown in Figure 1.

The structure consists of substrate silicon with a refractive index of 1.512, waveguide, which is silicon with a refractive index (1.521), MgF2, and silver layer thickness of 30 nm. The main goal is to enhance the stability of silver film and detect the best thickness that has the best resonance using two types of analytes: air and water.

This study suggested changing the thickness of silver to calculate the best resonance wavelength at each proposed thickness and the mode profile. A graphene layer was added with the thicknesses 1 nm, 3 nm, and 5 nm, the analyte's refractive index (1.1, 1.2, 1.3, and 1.333).

The simulations program was done by Lumerical Finite-Difference Eigenmode (FDE) mode-solving software. In addition, a mode calculator solver is available on the commercial software Lumerical Mode solutions, which can use different indices for both directions perpendicular to the propagation and calculate mode profile and resonance wavelength [30].

Inserting a buffer layer with an appropriate index and thickness allows phase matching between the waveguide mode and surface plasmonic wave. This is achieved in the presence of a superstrate medium with an index near that of a single buffer layer of magnesium fluoride. A suitable dielectric used for multilayer interference filters allowed mode coupling to be achieved. The film is weakly birefringent, and its optical properties do not vary significantly across the wavelength range of interest (550-800 nm) at the studied refractive index [18].

4. Results and Discussion

A two sensors structures were constructed in Lumerical FDE software. The first sensor contained a silver layer without Graphene, and the second was supported with a graphene layer. The first and the second sensor designs have a 30 nm thickness of silver material. Figure 2 shows that the effective refractive index changes with the analyte as well as the thickness of the silver metal (30 nm) without Graphene on SPR. The sharpness peak supported by the maximum loss is shown in Figure 2a. The silver layer and the broader peaks supported by the minimum loss are shown in Figure 2d. It can be seen that the Graphene was 5 nm thickness. Increasing any layer over the plasmonic layer will affect the loss.

Figure 3 shows the variation of center wavelength at different graphene thicknesses. The losses were maximum at t=0. This value is physically actual when nothing is deposited on the plasmonic material; any variation in thickness or refractive index will cause a recognizable losses value in this Figure.

The simulation output data is in Table 1, silver thickness, resonance wavelength, loss, sensitivity, FOM, and Refractive index of SPR without Graphene. These results show the maximum loss at 685 nm, which is 193.2 db. This sensor works in the visible range (550-800) nm and has a sensitivity of 140, and the FOM of the sensor was (2.27). When the refractive index is changing, the loss is changing, respectively. From the mode profile, notice that as the analyte's refractive index increases, the loss increases, which leads to an increase in the area through which the light passes and the cross-section of the field increases. This will maximize the loss with the increase of the field area, leading to an increase in the intensity and the Figure of merit.

Table 1: Simulation results at 30 nm silver plasmonic material with no graphene

Thickness (nm)	**resonance wavelength of (nm)**	**Sensitivity nm/RIU**	**FOM**	**Refractive index**
30	652.8		1.984	air
	661.4	105	1.9535	1.1
	670.9		2.086	1.2
	681.6	140	2.2544	1.3
	685.5		2.274	water

The variation of the graphene thickness can cause variation in sensitivity and FOM. The sensitivity will increase with the thickness of graphene layers. As the reflected index of the analyte was increased, this led to an increasing loss, which spread more formally in the electric field. This is described as if the cross-section of the field was increased. Moreover, when the field is increased, this decreases the sensitivity.

In the second sensor, which was designed with a silver layer and Graphene, the thickness of the silver layer was 30 nm while the thickness of Graphene was (1, 3, 5) nm, as listed in Table 2. It was noticed that with the increase of the thickness of Graphene leads to an increase in sensitivity. Moreover, a decrease in the loss and Figure of merit and increased resonance curve width were also observed. As a result, the sensitivity was 73.5 at 1 nm, 81.5 at 3nm, and 82 at 5 nm graphene.

The graphene-based sensor relies on the generation of the electric field near the surface or interface of the metal/graphene layer to improve the sensitivity of biosensors. This electric field is essential to separate the carriers or photo carriers and increase the sensor efficiency; Figure 4 shows the silver layer in air and water and silver/graphene in air and water. The electric field shows increasing significantly after adding the graphene layer.

Figure 5 shows the increasing electric field, reflecting the sensing region's sensitivity. In this Figure, adding the graphene layer at different thicknesses increases the electric field in the refractive index range. Increasing the electric field means the analyte's evanescent field is more than without a Graphene layer [26]. The added Graphene layer on the silver metal by different thicknesses refers to the effect on wavelength resonance and increased loss because the Graphene increases the absorption of analytic molecules. Also, an increase in the thickness of Graphene leads to sensitivity increasing gradually. Hence, increasing the thickness of Graphene is always recommended. It also increases the amount of light absorbed by the exact value of 2.3%. Graphene's optical absorption of 2.3% is always constant [12].

Table 2: Simulation results at 30 nm silver plasmonic material with different thicknesses of the Graphene

Thickness (nm)	The thickness of Graphene (nm)	Wavelength (nm)	Sensitivity	FOM	N
30	1	631.2		1.54	Air
		636.8	75.5 nm/RIU	1.544	1.1
		643.7		1.534	1.2
		651.5	76.6 nm/RIU	1.4759	1.3
		653.8		1.467	Water
30	3	770.5	81.5 nm/RIU	1.156	Air
		680.5		1.195	1.1
		688.9		1.1845	1.2
		696.8		1.0187	1.3
		699.7		0.969	Water
30	5	682.3		0.91	Air
		689	82 nm/RIU	0.8577	1.1
		695.7		0.844	1.2
		705.4		0.684	1.3
		707.5		0.6867	Water

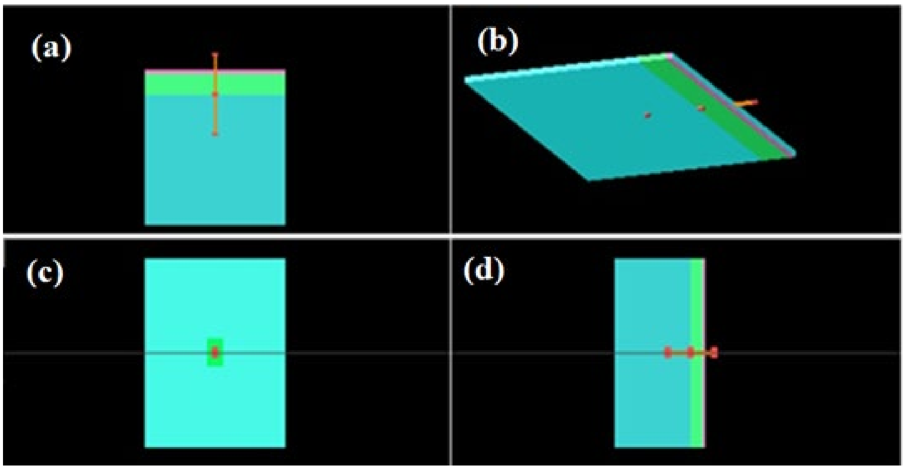

Figure 1: The proposed SPR sensor design: (a) afront view. (b) top view (c) left view. (d) right view

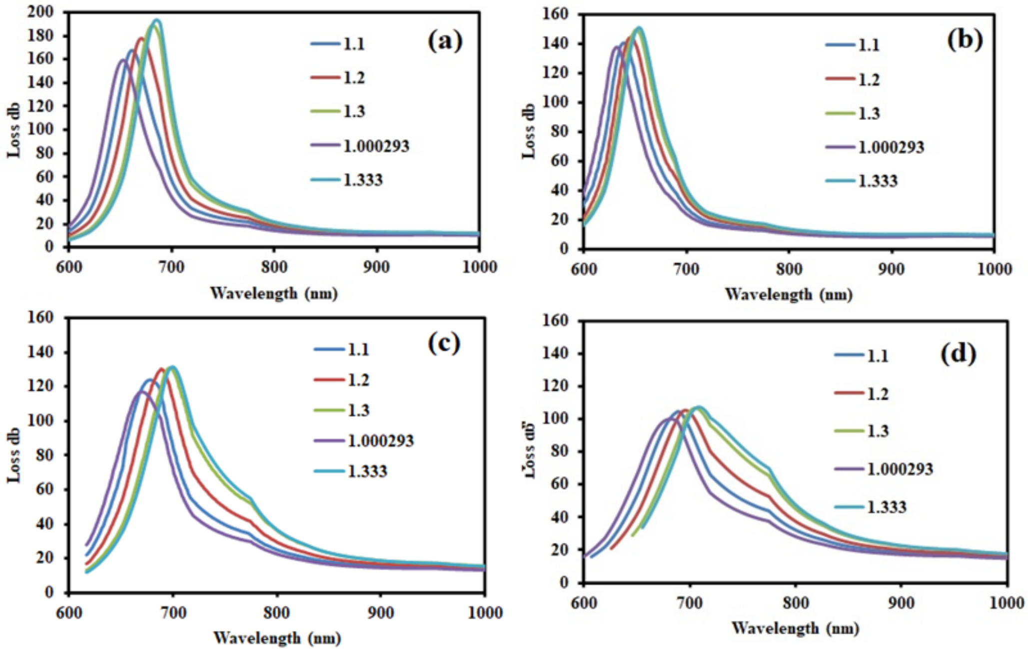

Figure 2: Analyte refractive index with thickness silver metal (30 nm) (a without graphene b) graphene 1 nm thickness (c graphene 3 nm thickness d) with graphene 5 nm thickness

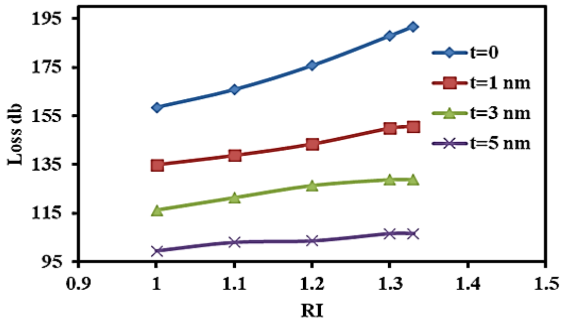

Figure 3: Center wavelength variation at different thickness

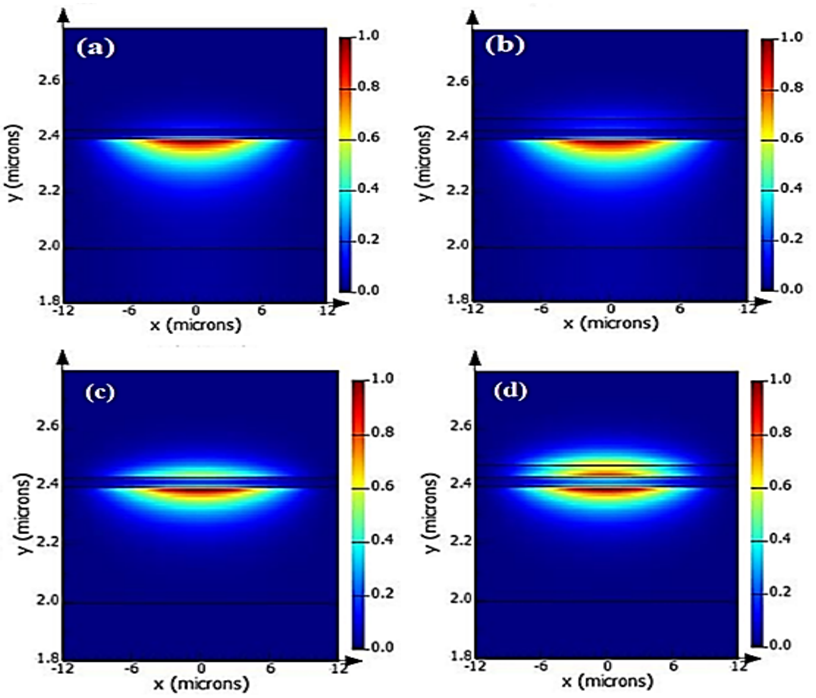

Figure 4: Silver layer: (a) Silver without Graphene in air. (b) Silver without Graphene in water. (c) Silver with Graphene in air. (d) Silver with Graphene in water

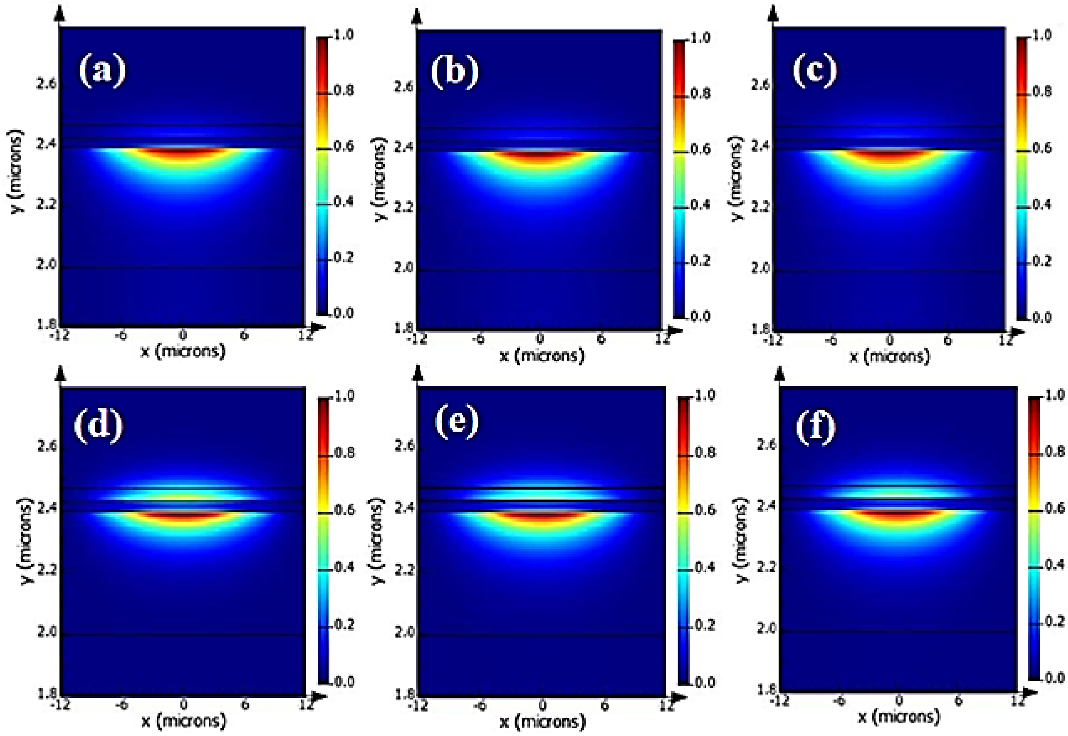

Figure 5: The increasing electric field: (a) Silver without Graphene in N=1.1. (b) Silver without Graphene in N=1.2. (c) Silver without Graphene in N=1.3. (d) Silver with graphene thickness of 1 nm and N=1.1. (e) Silver with graphene thickness of 3 nm. (f) Silver with graphene thickness of 5 nm

5. Conclusion

The current study developed a surface plasmon sensor model for Graphene with different thicknesses in different analytes (air, then 1.1, 1.2, 1.3, and water). The wavelength of resonance, loss, sensitivity, FOM, and Refractive index using Lumerical FDE were numerically calculated.

We can plot the effective change of refractive index of the analyte with a thickness of silver metal (30 nm) without Graphene on SPR and the effect change of refractive index of the analyte with a thickness of silver metal (30 nm) with Graphene (1, 3, and 5 nm) on SPR, respectively in this different analyte.

The SPR's electric field with and without the Graphene in air and water in thicknesses of (1, 3, and 5 nm) were investigated. The numerical data showed the differences in the electric field of SPR in the number of refractive indexes after applying the silver coating layer, and the performance parameters improved. Graphene has much promise, yet almost most of it is still unexplored. The fundamentals of graphene-based waveguides and devices were investigated. The aim is to work on various graphene-based practical uses like biosensors and Nanochips in the future.

Acknowledgment

The authors would like to thank the University of Technology, Baghdad, Iraq, for its support in the present work.

Author contribution

Conceptualization, Ali Abdulkhaleq Alwahib. and Amnh S. Hasan; methodology, Ali Abdulkhaleq Alwahib. and Amnh S. Hasan; software, Amnh S. Hasan; validation, Amnh S. Hasan; formal analysis, Amnh S. Hasan; investigation, Amnh S. Hasan; resources, Amnh S. Hasan; data curation, Amnh S. Hasan; writing—original draft preparation Ali Abdulkhaleq Alwahib. and Amnh S. Hasan; writing—review and editing, Ali Abdulkhaleq Alwahib; visualization, Ali Abdulkhaleq Alwahib; supervision, Razi J.Al-Azawi; project administration, Razi J.Al-Azawi; funding acquisition, Ali Abdulkhaleq Alwahib. All authors have read and agreed to the published version of the manuscript.

Funding

This research received no external funding.

Conflicts of interest

The authors declare no conflict of interest and the funders had no role in the study's design, in the collection, analyses, or interpretation of data, in the writing of the manuscript, or in the decision to publish the results.

References

[1] R. C. C. Jorgenson and S. S. S. Yee, A fiber-optic chemical sensor based on surface plasmon resonance, Sens. Actuators B Chem., 12 (1993) 213–220, https://doi.org/10.1016/0925-4005(93)80021-3

[2] R. C. Jorgenson, C. Jung, S. S. Yee, L. W. Burgess, Multi-wavelength surface plasmon resonance as an optical sensor for characterizing the complex refractive indices of chemical samples, Sens. Actuators B Chem.,14 (1993) 721–722.

[3] J. Homola, Optical fiber sensor based on surface plasmon excitation, Sens. Actuators B Chem., 29 (1995) 401–405. https://doi.org/10.1016/0925-4005(95)01714-3

[4] B. Liedberg, C. Nylander, I. Lunström, Surface plasmon resonance for gas detection and biosensing, Sens. Actuators, 4 (1983) 299–304. https://doi.org/10.1016/0250-6874(83)85036-7

[5] D. R. Shankaran, K. V. Gobi, N. Miura, Recent advancements in surface plasmon resonance immunosensors for detection of small molecules of biomedical, food and environmental interest, Sensors. Actuators. B Chem., 121 (2007) 158–177. https://doi.org/10.1016/j.snb.2006.09.014

[6] S. A. Maier, Plasmonics: Fundamentals and applications, Plasmon. Fundam. Appl., 5 (2007) 1–223, 2007. https://doi.org/10.1007/0-387-37825-1

[7] K. Matsubara, S. Kawata, S. Minami, Optical chemical sensor based on surface plasmon measurement, Appl. Opt., 27 (1988) 1160 -1163. https://doi.org/10.1364/ao.27.001160

[8] A. Otto., Excitation of nonradiative surface plasma waves in silver by the method of frustrated total reflection, Zeitschrift für Phys., 216 (1968) 398–410. https://doi.org/10.1007/BF01391532

[9] R. D. Harris , J. S. Wilkinson, Waveguide surface plasmon resonance sensors, Sensors Actuators B. Chem., 29 (1995) 261–267. https://doi.org/10.1016/0925-4005(95)01692-9

[10] R. H. Ritchie, E. T. Arakawa, J. J. Cowan, and R. N. Hamm, Surface-plasmon resonance effect in grating diffraction, Phys. Rev. Lett., 21 (1968) 1530–1533. https://doi.org/10.1103/PhysRevLett.21.1530

[11] D. J. Webb, Research activities arising from the University of Kent, Photonic. Sens., 1 (2011) 140–151. https://doi.org/10.1007/s13320-011-0030-7

[12] S. Thongrattanasiri, F. H. L. Koppens, F. J. García De Abajo, Complete optical absorption in periodically patterned Graphene, Phys. Rev. Lett., 108 (2012) 1–5. https://doi.org/10.1103/PhysRevLett.108.047401

[13] M. Piliarik, H. Vaisocherová, J. Homola, A new surface plasmon resonance sensor for high-throughput screening applications, Biosens. Bioelectron., 20 (2005) 2104–2110. https://doi.org/10.1016/j.bios.2004.09.025

[14] Q. Duan, Y. Liu, S. Chang, H. Chen, J. H. Chen, Surface plasmonic sensors: Sensing mechanism and recent applications, Sensors, 21 (2021) 12–25. https://doi.org/10.3390/s21165262

[15] S. A. Taya, M. M. Shabat, H. M. Khalil, Enhancement of sensitivity in optical waveguide sensors using left-handed materials, Optik , 120 (2009) 504–508. https://doi.org/10.1016/j.ijleo.2007.12.001

[16] S. K. Selvaraja, P. Sethi, Review on Optical Waveguides, Emerg. Waveguide Technol., 1 (2018) 22–31.

[17] A. L. Washburn , R. C. Bailey, Photonics-on-a-chip: Recent advances in integrated waveguides as enabling detection elements for real-world, lab-on-a-chip biosensing applications, Analyst, 136 (2011) 227–236. https://doi.org/10.1039/c0an00449a

[18] P. Kozma, F. Kehl, E. E. Förster, C. Stamm, F. F. Bier, Integrated planar optical waveguide interferometer biosensors: A comparative review, Biosens. Bioelectron., 58 (2014) 287–307. https://doi.org/10.1016/j.bios.2014.02.049

[19] K. J. Ebeling, Strip Waveguides, in Integrated Optoelectronics, Springer.(1993) 75–108.

[20] V. I. Nalivaiko M. A. Ponomareva, Comparison of Characteristics of Waveguide Refractometric Sensors, Opt. Spectrosc., 127 (2019) 1128–1132. https://doi.org/10.1134/S0030400X19120154

[21] M. J. Allen, V. C. Tung, R. B. Kaner, Honeycomb carbon: A review of Graphene, Chem. Rev., 110 (2010) 132–145. https://doi.org/10.1021/cr900070d

[22] M. Bruna , S. Borini, Optical constants of graphene layers in the visible range, Appl. Phys. Lett., 94 (2009) 31901.

[23] B. H. Ong, X. Yuan, S. C. Tjin, Bimetallic silver-gold film waveguide surface plasmon resonance sensor, Integr. Opt. Devices., 6123 (2006) 61230B. https://doi.org/10.1117/12.644028

[24] E. K. Akowuah, T. Gorman, S. Haxha, Design and optimization of a novel surface plasmon resonance biosensor based on Otto configuration, Opt. Express., 17 (2009) 23511- 23521. https://doi.org/10.1364/oe.17.023511

[25] S. Micloş, D. Savastru, A. Popescu, L. Başchir, R. Savastru, Simulation of surface plasmon propagation in planar waveguides, Ser. A Appl. Math. Phys., 78 (2016) 283–290.

[26] L. Ji, S. Yang, R. Shi, Y. Fu, J. Su, C. Wu, Polymer Waveguide Coupled Surface Plasmon Refractive Index Sensor: A Theoretical Study, Photonic Sens.,10 (2020) 353–363. https://doi.org/10.1007/s13320-020-0589-y

[27] L. Kong, J. Lv, Q. Gu, Y. Ying, X. Jiang, G. Si, Sensitivity-enhanced spr sensor based on Graphene and subwavelength silver gratings, Nanomater., 10 (2020) 1–12. https://doi.org/10.3390/nano10112125

[28] H. K. Rouf, T. Haque, Sensitivity Enhancement of Graphene-MoSe2–Based SPR Sensor Using Ti Adhesion Layer for Detecting Biological Analytes, Plasmonics , 16 (2021) 1945–1954 . https://doi.org/10.1007/s11468-021-01445-2

[29] C. R. Lavers, J. S. Wilkinson, A waveguide-coupled surface-plasmon sensor for an aqueous environment, Sens. Actuators B Chem., 22 (1994) 75–81. https://doi.org/10.1016/0925-4005(94)01260-1

[30] M. Riaz, S. K. Earles, A. Kadhim, A. Azzahrani, Computer analysis of microcrystalline silicon hetero-junction solar cell with lumerical FDTD/DEVICE, Int. J. Comput. Mater. Sci. Eng., 6 (2017) 12–22. https://doi.org/10.1142/S2047684117500178